© 2014. Published by The Company of Biologists Ltd | Development (2014) 141, 1572-1579 doi:10.1242/dev.100305

RESEARCH ARTICLE

Pitx2c ensures habenular asymmetry by restricting parapineal cell number

Laurence Garric[1,2], Brice Ronsin[1,2], Myriam Roussigné[1,2], Sabrina Booton[3], Joshua T. Gamse[3], Pascale Dufourcq[1,2,*] and Patrick Blader[1,2,*]

ABSTRACT

Left-right (L/R) asymmetries in the brain are thought to underlie lateralised cognitive functions. Understanding how neuroanatomical asymmetries are established has been achieved through the study of the zebrafish epithalamus. Morphological symmetry in the epithalamus is broken by leftward migration of the parapineal, which is required for the subsequent elaboration of left habenular identity; the habenular nuclei flank the midline and show L/R asymmetries in marker expression and connectivity. The Nodal target *pitx2c* is expressed in the left epithalamus, but nothing is known about its role during the establishment of asymmetry in the brain. We show that abrogating Pitx2c function leads to the right habenula adopting aspects of left character, and to an increase in parapineal cell numbers. Parapineal ablation in Pitx2c loss of function results in right habenular isomerism, indicating that the parapineal is required for the left character detected in the right habenula in this context. Partial parapineal ablation in the absence of Pitx2c, however, reduces the number of parapineal cells to wild-type levels and restores habenular asymmetry. We provide evidence suggesting that antagonism between Nodal and Pitx2c activities sets an upper limit on parapineal cell numbers. We conclude that restricting parapineal cell number is crucial for the correct elaboration of epithalamic asymmetry.

KEY WORDS: Nodal, Pitx2, Epithalamus, Left-right, Parapineal, Zebrafish

INTRODUCTION

The epithalamus is composed of the left and right habenulae, and the pineal complex, which is itself composed of the pineal gland and the parapineal nucleus (Concha and Wilson, 2001). Although the habenulae link the anterior forebrain to the ventral midbrain, the pineal complex is a photoreceptive structure involved in regulating circadian rhythms. In zebrafish, the epithalamus is highly asymmetric along the left-right (L/R) axis (for a review, see Roussigné et al., 2012). Indeed, the habenulae display a variety of L/R differences in the expression of various markers and transgenes. The pineal complex also shows prominent L/R asymmetry, with the parapineal being located almost exclusively in a left-sided position at later stages. The parapineal does not form on the left, however, but is derived from the anterior/medial region of the pineal that delaminates and migrates leftward. During development, the parapineal is crucial for the elaboration of left habenular character, as laser ablation prior to its migration results in both the left and right habenula adopting largely 'right' characteristics (Concha et al., 2003; Gamse et al., 2003; Aizawa et al., 2005; Bianco et al., 2008).

The signalling pathways underlying the establishment of epithalamic asymmetry in the zebrafish are being unravelled. For example, a TGFβ family member related to mammalian Nodal, Cyclops/Ndr2, is transiently expressed in the left epithalamus where it is required for biasing parapineal migration to the left (Concha et al., 2000; Liang et al., 2000). In the absence of unilateral Nodal activity, however, asymmetry develops in the epithalamus but with randomised laterality; the parapineal migrates to the left or right with a similar frequency and the habenulae develop asymmetry concordant with the handedness of the parapineal. Conversely, in embryos homozygous for a weak allele of *acerabellar* (*ace*), a *fgf8* mutant, the parapineal develops but remains at the midline and the habenulae develop symmetrically (Regan et al., 2009). The intracellular factors involved in the development of epithalamic asymmetry, however, remain largely unknown.

The *Pitx2* gene encodes a homeobox transcription factor that is a target of Nodal signalling, and that is mutated in individuals with Axenfeld-Rieger syndrome who display ocular and craniofacial abnormalities (Semina et al., 1996; Shiratori et al., 2001). In mouse, *Pitx2* mutants display phenotypes that include alterations in heart positioning and right isomerisation of the lungs (Kitamura et al., 1999; Lin et al., 1999; Lu et al., 1999; Liu et al., 2001). In zebrafish embryos, two isoforms of Pitx2 are generated from a single gene through the use of distinct promoters. The expression patterns of the two isoforms are largely similar, but differences exist in structures that display asymmetries along the left-right axis; the *pitx2a* isoform is expressed in the left heart field and the *pitx2c* is expressed in the gut and in the left dorsal diencephalon (Essner et al., 2000). Although studies have shown that concomitant knock-down of both the 2a and 2c isoforms phenocopies some aspects of Axenfeld-Rieger syndrome, nothing is known about a role for *pitx2c* in the development of L/R asymmetry in the zebrafish epithalamus (Bohnsack et al., 2012; Liu and Semina, 2012).

Here, we show that there is an increase in parapineal cell number in the *pitx2c* loss-of-function context that correlates with the acquisition of aspects of left character in the right habenula. Artificially restricting the number of parapineal cells in this context rescues the habenular phenotype. We propose that restricting parapineal cell number is crucial for the correct elaboration of asymmetry in the epithalamus and that Pitx2c participates in this process.

RESULTS

pitx2c morphant embryos display partial left isomerism of the habenulae

To address a potential role for Pitx2 in the elaboration of L/R asymmetry in the developing zebrafish brain, we employed a

[1]Université de Toulouse, UPS, Centre de Biologie du Développement (CBD), 118 route de Narbonne, F-31062 Toulouse, France. [2]CNRS, CBD UMR 5547, F-31062 Toulouse, France. [3]Department of Biological Sciences, Vanderbilt University, Nashville, TN 37205, USA.

*Authors for correspondence (pascale.dufourcq@univ-tlse3.fr; patrick.blader@univ-tlse3.fr)

Received 20 June 2013; Accepted 7 February 2014

Development (2014) doi:10.1242/dev.100305

morpholino knockdown strategy that targets the Pitx2c isoform specifically. Morphant embryos develop in a manner that is globally indistinguishable from wild-type and control morphants (data not shown). Furthermore, the asymmetric expression of the Nodal pathway genes is unchanged, suggesting that early events in the establishment of L/R asymmetry are unaffected (supplementary material Fig. S1) (Thisse and Thisse, 1999; Essner et al., 2000; Long et al., 2003).

Next, we analysed the expression of genes displaying L/R asymmetric patterns in the habenulae in *pitx2c* morphants. As previously described, the expression of the potassium channel tetramerization domain containing 8 (*kctd8/dexter*) gene is broader in the right than the left habenula of wild-type embryos at 72 hours post-fertilisation (hpf) and this pattern remains unchanged in embryos injected with either a control morpholino or morpholinos targeting *pitx2c* (Fig. 1A-C′,G) (Gamse et al., 2005); the expression of a second right asymmetric potassium channel tetramerization domain containing gene, *kctd12.2*, is similarly unaffected (supplementary material Fig. S2A-C). Conversely, although in wild-type and control morphant embryos the habenular expression volumes of a third Kctd gene, *kctd12.1*/*leftover*, are asymmetric with broader expression in the left habenula at 72 hpf, in *pitx2c* morphant embryos the asymmetry index is significantly reduced (Fig. 1D′,E′,F′,G) (Gamse et al., 2003). However, although *pitx2c* is expressed exclusively in the left dorsal diencephalon, the shift toward symmetry in *pitx2c* morphant embryos is the result of an expansion of *kctd12.1* expression in the right rather than a decrease of expression in the left habenula (Fig. 1E versus Fig. 1D,F). Similarly, a habenular neuropil of left character appears in the right habenula in *pitx2c* morphants (supplementary material Fig. S2D,D′). Not all markers expressed preferentially in the left epithalamus behave in a more symmetric manner in the *pitx2c* knockdown context; *nrp1a* expression remains robustly asymmetric (supplementary material Fig. S2E-G). Finally, expression of the pan-habenular marker *brn3a* is unaffected in *pitx2c* morphants at 72 hpf, suggesting that overall habenular size is unchanged in the absence of Pitx2c function (supplementary material Fig. S2H-J) (Aizawa et al., 2005; Roussigné et al., 2009). Taken together, these results indicate that Pitx2c is required for the establishment of a subset of L/R habenular asymmetries.

Parapineal cell numbers are increased in *pitx2c* morphant embryos

The elaboration of left habenular character requires input from the parapineal (Concha et al., 2003; Gamse et al., 2003). Moreover, in

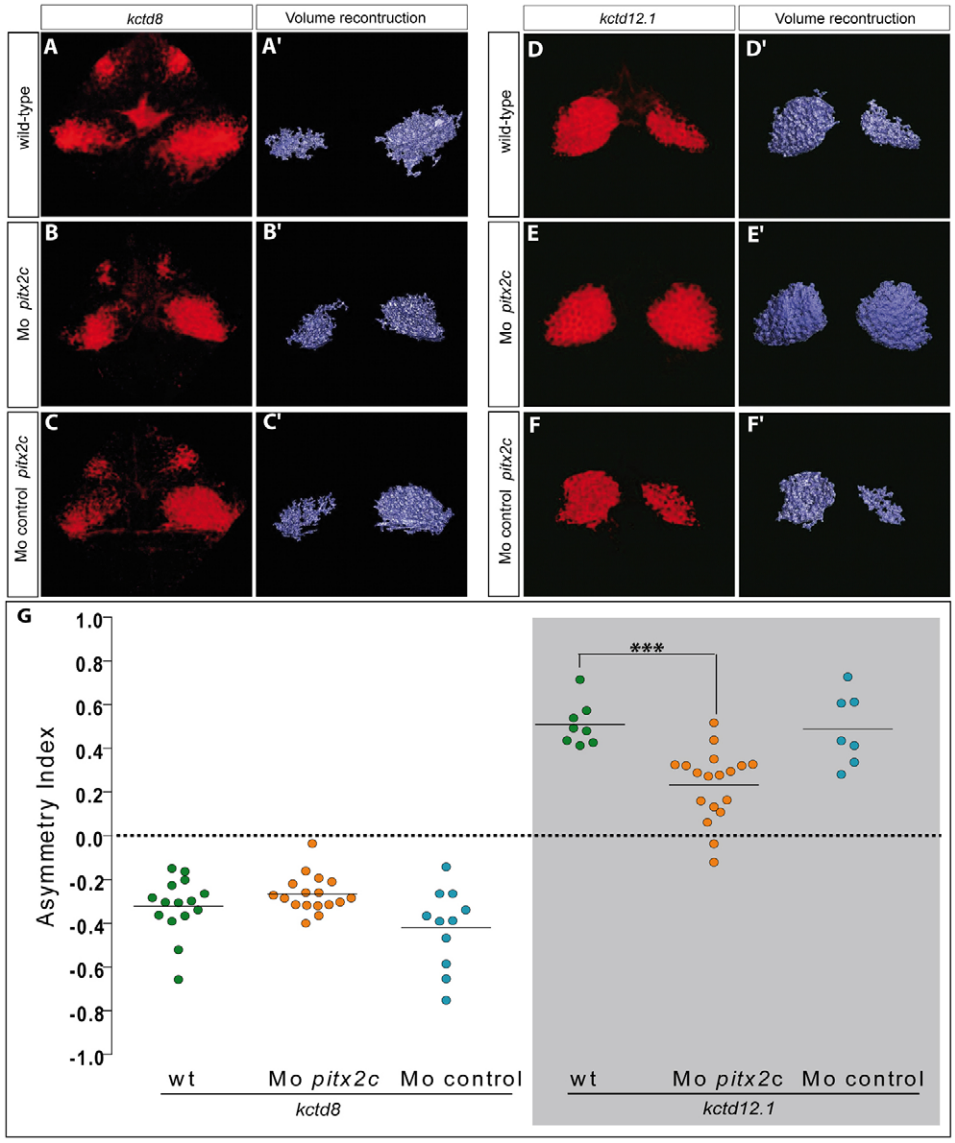

Fig. 1. Partial left isomerisation in *pitx2c* morphants. (A-C) Single confocal sections of the epithalamus showing *in situ* hybridisation against *kctd8* in wild-type, *pitx2c* morphant and control morphant embryos at 72 hpf. No differences are detected between the different contexts. (A′-C′) Three-dimensional renderings of volumes of *kctd8* expression in the habenulae of the respective confocal acquisition sets. (D-F) Single confocal sections of the epithalamus showing *in situ* hybridisation against *kctd12.1* in wild-type, *pitx2c* morphant and control morphant embryos at 72 hpf. *pitx2c* morphants display broader expression of *kctd12.1* in the right habenula than either of the control contexts. (D′-F′) Three-dimensional renderings of volumes of *kctd12.1* expression in the habenulae of the respective confocal acquisition sets. (G) Asymmetry index (AI) with regard to the volumes of *kctd8* or *kctd12.1* expression for individual wild-type (wt), control or *pitx2c* morphant embryos. Horizontal black line represents the median AI for each context and the dotted line indicates symmetry. Only the AI for the expression of *kctd12.1* in *pitx2c* morphants is significantly more symmetric than control conditions; ***P<0.001 using a t-test. Embryos are viewed dorsally with the anterior to the top.

Development (2014) doi:10.1242/dev.100305

some mutant contexts, cases of left isomerism of *kctd12.1* expression are associated with a duplication of the parapineal on the right side of the dorsal diencephalon (Gamse et al., 2003). We, thus, asked whether the partial left habenular isomerism we detect in *pitx2c* morphant embryos correlates with changes in the development or migratory behaviour of the parapineal.

The expression of parapineal markers, such as *gfi1.2* and *Et(krt4:EGFP)*^{sqet11}, is detected in morphants at 72 hpf, indicating that the parapineal is formed in the *pitx2c* knock-down context (Fig. 2A,B; supplementary material Fig. S3A,B) (Dufourcq et al., 2004; Choo et al., 2006). Furthermore, reduction of *pitx2c* function does not affect the orientation of parapineal migration. We did find, however, that expression of the *Tg(foxd3:GFP)*^{zf15} transgene appears in parapineal cells with an approximately 12-hour delay in *pitx2c* morphants relative to wild type (Fig. 2D-D‴ versus Fig. 2E-E‴); robust expression of GFP from the *Tg(foxd3:GFP)*^{zf15} is detected at later stages in *pitx2c* morphants (data not shown). These data suggest that Pitx2c is required for the correct schedule of neural specification in the parapineal.

We also found that the number of cells in the parapineal in *pitx2c* morphants differs from wild-type embryos. Indeed, although 17±0.94 and 9±0.75 cells are labelled respectively, with *gfi1.2* and *Et(krt4:EGFP)*^{sqet11}, in controls a significantly larger number of cells are labelled in *pitx2c* morphants with these markers (25±1.59 and 12±1.57 cells; Fig. 2C; supplementary material Fig. S3). To address the origin of the increased number of parapineal cells, we performed time-lapse confocal analysis on wild-type and *pitx2c* morphant embryos (Fig. 2D-E‴). At 24 hpf, a stage just prior to parapineal migration, no difference in the number of parapineal cells was detected between wild-type and *pitx2c* morphant embryos, indicating that reducing *pitx2c* function does not influence the initial number of parapineal cells (Fig. 2D,E,F). As the parapineal migrates, however, supernumerary cell divisions lead to a significant increase in the number of cells per parapineal in morphant versus control embryos (Fig. 2F; supplementary material Movie 1 versus Movies 2 and 3). The extra cell divisions tend to occur during the first 6 hours of migration but can be detected up to 14 hours after migration is initiated. No signs of apoptosis of parapineal neurons was noted in our time-lapse data sets, suggesting that cell death does not eliminate parapineal neurons in wild-type embryos. Furthermore, all parapineal cells identified at the end of the time-lapse datasets are derived from cell divisions of the initially delaminated cell population, indicating that supernumerary cells do not join the parapineal during its migration from elsewhere in the epithalamus. In conclusion, our data indicate that Pitx2c limits the mitotic capacity of parapineal cells once they have been determined.

Previous studies have shown that habanular asymmetry is established in embryos lacking Nodal signalling in the epithalamus, despite them failing to express *pitx2c* (Concha et al., 2000; Liang et al., 2000). Furthermore, treatment of embryos from 16 hpf with SB431542, a small molecule inhibitor of Nodal signalling, blocks *pitx2c* expression in the epithalamus but does not result in an enlarged parapineal (Fig. 3A-C). One explanation for these

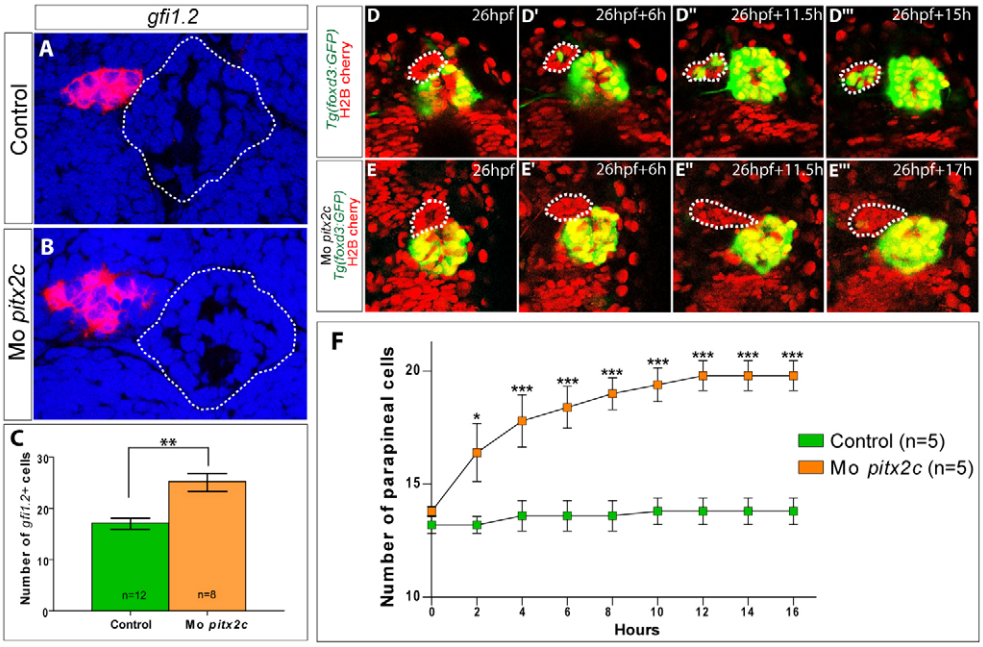

Fig. 2. *pitx2c* morphants display larger parapineals. (A,B) Single confocal sections of the pineal complex showing *in situ* hybridisation against *gfi1.2* in control and *pitx2c* morphant embryos at 72 hpf. The outline of the pineal gland is highlighted with a dotted line. (C) Counts of cell expressing *gfi1.2* in control and *pitx2c* morphants. The number of *gfi1.2*-positive cells is significantly increased in the morphant context; ***P*<0.01 using a *t*-test. Error bars represent s.e.m. (D-D‴) Single confocal sections extracted from a time-lapse series showing the migrating parapineal (indicated with a dotted line) in a *Tg(foxd3:GFP)*^{zf15} embryo; nuclei are labelled in red with Histone2B:RFP. At 24 hpf (D), the parapineal has only just delaminated from the anterior region of the pineal complex. Leftward migration is clearly engaged at 6 hours (D′) and continues throughout the analysis (D″,D‴). Time after the initiation of the analysis is indicated on each frame. (E-E‴) Single confocal sections extracted from a time-lapse series showing the migrating parapineal (indicated with a dotted line) in a *pitx2c* morphant embryo carrying the *Tg(foxd3:GFP)*^{zf15} transgene; nuclei are labelled in red with Histone2B:RFP. As in wild-type siblings, *pitx2c* morphant parapineals have migrated to the left at 6 hours. Time after the initiation of the analysis is indicated on each frame. (F) Numbers of cells in the parapineal during migration in wild-type (green) and *pitx2c* morphant embryos (orange). A statistically significant difference in parapineal cell numbers is detected in the morphant versus the control as early as 2 hours into the time-lapse datasets. **P*>0.1; ****P*<0.0.001 using a two-way repeated measures ANOVA test. Error bars represent s.e.m. Embryos are viewed dorsally with the anterior towards the top.

Development (2014) doi:10.1242/dev.100305

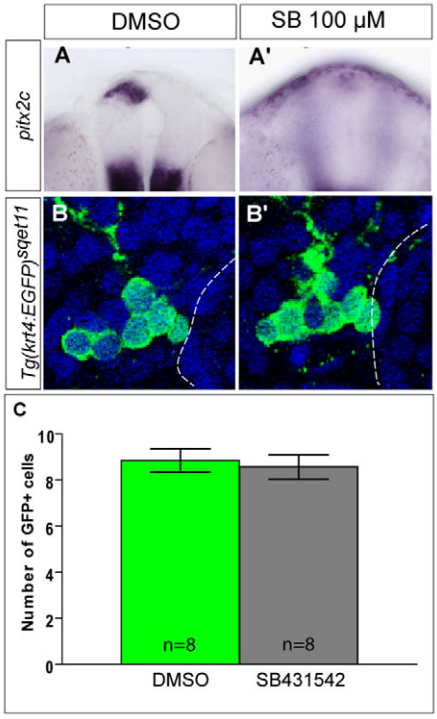

Fig. 3. Parapineal cell numbers are unaffected in the absence of epithalamic Nodal signalling. (A,A′) Frontal view of the epithalamus showing *in situ* hybridisation against *pitx2c* at 24 hpf in mock-treated embryos (A) or those treated with 100 μM SB431542 (A′). (B,B′) Single confocal sections of the parapineal showing the expression of GFP from the *Et(krt4:EGFP)*^{sqet11} transgene in mock-treated embryos (B) or those treated with 100 μM SB431542 (B′). The outline of the pineal gland is highlighted with a dotted line. (C) Counts of cell expressing the *Et(krt4:EGFP)*^{sqet11} transgene in mock-treated and SB431542-treated embryos. The number of GFP-positive cells is unaffected by treatment with SB431542. Error bars represent s.d.

paradoxical results could be that Nodal signalling promotes an increase in cell number in the parapineal and that Pitx2c acts to impede this activity; in the absence of epithalamic Nodal activity this level of control would no longer be required. If the threshold of Nodal signalling needed to promote increased parapineal cell number is higher than that needed to drive *pitx2c* expression then suboptimal levels of Nodal signalling should lead to a reduction in the number of parapineal cells. To explore this, we modulated Nodal signalling with varying concentrations of SB431542 and monitored parapineal cell number. Mock treatment with DMSO or treatment with 100 or 75 μM SB431542 had no effect on parapineal size (Fig. 4E). Conversely, embryos treated with SB431542 at 50 μM show a significant reduction in the number of *gfi1.2*$^{+}$ parapineal cells (Fig. 4A,B,E); treatment with 25 μM SB431542 had a small but statistically insignificant effect on parapineal cell number (Fig. 4E). The various SB431542 treatment regimes have a graded effect on the expression of *pitx2c* at 24 hpf (supplementary material Fig. S4). If residual Pitx2c restricts the number of parapineal cells at suboptimum levels of Nodal activity, knocking down Pitx2c function in this context should restore wild-type cell counts. Indeed, although *pitx2c* morpholino injection into DMSO-treated embryos leads to an increase in parapineal cell number similar to that described above, *pitx2c* morphant embryos treated with 50 μM SB431542 display wild-type numbers of parapineal cells (Fig. 4C,D,F). From these results, we propose that antagonism between Nodal and Pitx2c is involved in setting an upper limit of parapineal cell number (Fig. 4G).

Restricting parapineal cell numbers in *pitx2c* morphants rescues habenular asymmetry

To begin to address whether the partial left habenular isomerism detected in *pitx2c* morphants is due to the concomitant changes detected in the parapineal, we performed parapineal ablations. In wild-type embryos, ablation of parapineal precursors prior to their migration leads to a ‘double right’ pattern of *kctd12.1* expression (Fig. 5A,B) (Concha et al., 2003; Gamse et al., 2003); volumetric analysis shows that such ablations result in symmetric *kctd12.1* expression pattern (Fig. 5A′,B′,E). Ablation of either the left or right half of the parapineal anlage prior to migration reduces parapineal cell numbers but had no effect on the resulting asymmetric development of the habenulae (Fig. 5C-D′,E,J) (Concha et al., 2003). Whereas a ‘double left’ pattern of *kctd12.1* expression is detected in *pitx2c* morphants, complete ablation of parapineal precursors in this context results in a ‘double right’ *kctd12.1* phenotype (Fig. 5E-G′). Thus, in *pitx2c* morphants the expansion of left character in the right habenula seems to require the parapineal.

If the increase in parapineal cell number underlies the appearance of left character in the right habenula in *pitx2c* morphants, we hypothesised that reducing it in this context should rescue habenular asymmetry. For this, we performed partial ablations of parapineal precursors in the *pitx2c* morphant context. Such ablations result in parapineals whose cell number falls within the range sufficient for imposing correct habenular asymmetry in wild-type embryos (Fig. 5J); unlike partial ablation in wild-type embryos, however, more parapineal cells remain after ablation of the right than the left parapineal anlage in *pitx2c* morphants (Fig. 5J). Examination of the expression of *kctd12.1* indicates that L/R asymmetry is efficiently restored in morphant embryos where the parapineal has been partially ablated (Fig. 5E,H-I′). Taken together, our results suggest that Pitx2c restricts the number of cell of the parapineal and that this appears essential for the correct elaboration of habenular asymmetry.

DISCUSSION

Elaboration of epithalamic asymmetry requires reciprocal interactions between the anlage of the left habenula and the parapineal (for a review, see Roussigné et al., 2012). Previously, laser ablation studies suggest that there is a minimum parapineal cell number required for the acquisition of left habenular character (Concha et al., 2003; Gamse et al., 2003). Here, we provide the first evidence that setting an upper limit on parapineal cell number is equally important. Our results reveal one mechanism for restricting the number of parapineal cells involves Pitx2c.

Abrogation of Pitx2c function leads to an increase in parapineal cell number and a concomitant expansion of aspects of left character in the right habenula, but where and when Pitx2c acts is unknown. Although formal proof is lacking, there are several reasons to believe that the role of Pitx2c on parapineal cell numbers is achieved via an autonomous function in the left epithalamus. First, the expression of the *pitx2a* isoform overlaps extensively both spatially and temporally with that of *pitx2c* in most tissues, including the ventral diencephalon, and previous studies suggest that the two proteins are largely functionally redundant (Essner et al., 2000). Such redundancy does not exist in the epithalamus, however, as only the *pitx2c* isoform is expressed in this brain region. Second, with the exception of the epithalamus, the expression of *pitx2c* is symmetric in the brain whereas the effects we describe appear to be unilateral. Indeed, the results from our partial ablation studies suggest that

Development (2014) doi:10.1242/dev.100305

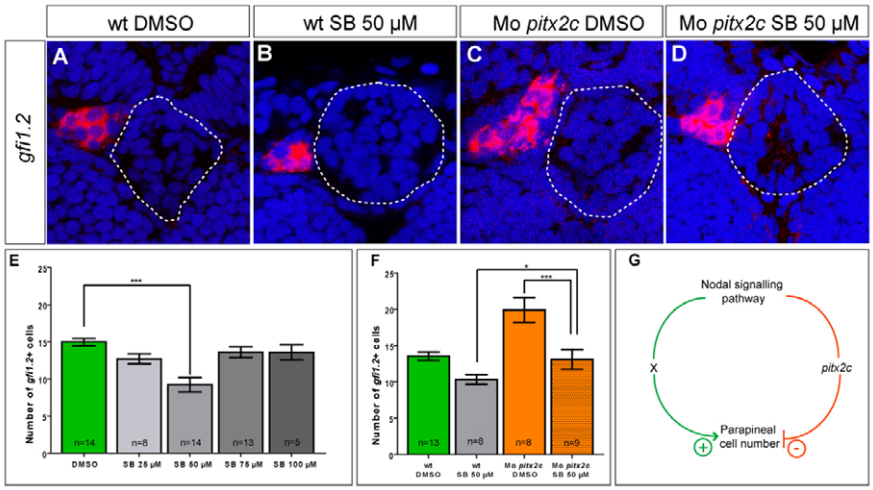

Fig. 4. Suboptimal Nodal signalling reduces parapineal cell number. (A-D) Single confocal sections of the pineal complex showing *in situ* hybridisation against *gfi1.2* in mock-treated, 50 µM SB431542-treated, mock-treated/*pitx2c* morphant and 50 µM SB431542-treated/*pitx2c* morphant embryos at 72 hpf. The outline of the pineal gland is highlighted with a dotted line. (E) Counts of cells expressing *gfi1.2* in mock-treated and SB431542-treated embryos. The number of *gfi1.2*-positive cells is significantly decreased only when embryos are treated with 50 µM SB431542; ***P<0.0.001 using a *t*-test. Error bars represent s.e.m. (F) Counts of cells expressing *gfi1.2* in mock-treated and SB431542-treated embryos injected with *pitx2c* morpholino. Whereas DMSO-treated morphant embryos leads to an increase in parapineal cell number, morphants embryos treated with 50 µM of SB431542 display wild-type numbers of parapineal cells; *P<0.05, ***P<0.0.001 using a *t*-test. Error bars represent s.e.m. (G) Model for the antagonism between Nodal and Pitx2c. Whereas Nodal activates *pitx2c* expression that subsequently limits parapineal cell numbers, in parallel a second target of Nodal signalling (X) promotes an increase in parapineal cell numbers. The balance between these two Nodal effectors provides fine control over the maximum cell number of the parapineal.

abrogation of Pitx2c function affects left parapineal precursors preferentially; although ablation of the left or right half of the parapineal anlage in wild-type embryos results in a similar number of residual parapineal cells being present, in the *pitx2c* morphant context statistically more residual parapineal cells are found if the right half of the parapineal anlage is ablated rather than the left half. An autonomous role for Pitx2c in left parapineal progenitors is also supported by the pattern of expression of *pitx2c*, which overlaps with these cells prior to parapineal migration (Liang et al., 2000). Further experiments, using conditional loss-of-function techniques such as photo-morpholinos, will be needed to address this issue in more detail.

Our results suggest that Pitx2c function restricts the mitotic capacity of parapineal cells during migration. How this restriction is achieved in molecular terms, however, remains unclear. Indeed, the best-known Pitx2 targets would appear to increase cell division and, as such, loss of Pitx2c would be expected to reduce the number of mitoses (Kioussi et al., 2002; Baek et al., 2003); Pitx2 is overexpressed in many cancers and is generally thought to promote cell proliferation. Recent proteomic and transcriptomic approaches have produced datasets of potential interactors and novel targets of Pitx2 from a variety of different cell types, including those affected in individuals with Axenfeld-Rieger syndrome, but the pertinence of these with respect to asymmetric development in the epithalamus remains to be determined (Huang et al., 2010; Paylakhi et al., 2011). The apparent antagonistic activities of Nodal and Pitx2c on parapineal cell numbers could perhaps provide clues. For example, Nodal and Pitx2c might regulate genes involved in cell-cycle progression, but in opposite fashions. Unfortunately, pertinent targets of Nodal signalling in the epithalamus other than *pitx2c* itself and *lefty1* are lacking. A final possibility would be that Pitx2c antagonises transduction of Nodal signals. Although Lefty1 is itself a feedback inhibitor of Nodal signalling, it is unlikely to act downstream of Pitx2c as we have shown that mopholino knock-down of *pitx2c* does not affect its expression.

Last, it is not obvious whether the increase in parapineal cell number in the absence of Pitx2c is the sole explanation for the effect on habenular asymmetry. Another explanation would be that the parapineal remains at the midline longer in *pitx2c* morphants, leaving it time to impose left character on the right habenula. For two reasons, however, we believe that this is unlikely. First, although in some *pitx2c* morphant embryos the parapineal appears to spend more time at the midline prior to migrating, this is not always the case. Second, genetic contexts have been reported in which there is a significant delay in parapineal migration without a concomitant effect on the acquisition of left and right habenular identity. For example, homozygous *one-eyed pinhead* mutant embryos in which the requirement for Oep during early developmental stages has been rescued – known as *Roep* embryos – display a significant delay in parapineal migration without the expansion of left character in the right habenula (Gamse et al., 2002; Gamse et al., 2003); the parapineal of 17% of *Roep* embryos remains at the midline until at least 48 hpf with no undue effect on the asymmetry in the expression of *kctd12.1* at later stages. Finally, reducing Pitx2c activity might sensitise the right habenula to parapineal influence. This is counter-intuitive, however, as *pitx2c* expression is limited to the left epithalamus. Furthermore, restoring wild-type parapineal cell numbers by laser ablation efficiently restores habenular asymmetry. We, therefore, favour the idea that the increase in parapineal cell number increases the capacity of the parapineal to emit signals that impose left habenular identity even across the dorsal midline. However, it remains unresolved why the right habenula adopts only a specific aspect of left character when Pitx2c activity is abrogated.

Conclusions

Pitx2 is a canonical Nodal target that has been implicated in the establishment of various aspects of L/R asymmetry in a variety of model systems. Here, we provide the evidence that Pitx2c is involved in limiting parapineal cell number during the establishment

Development (2014) doi:10.1242/dev.100305

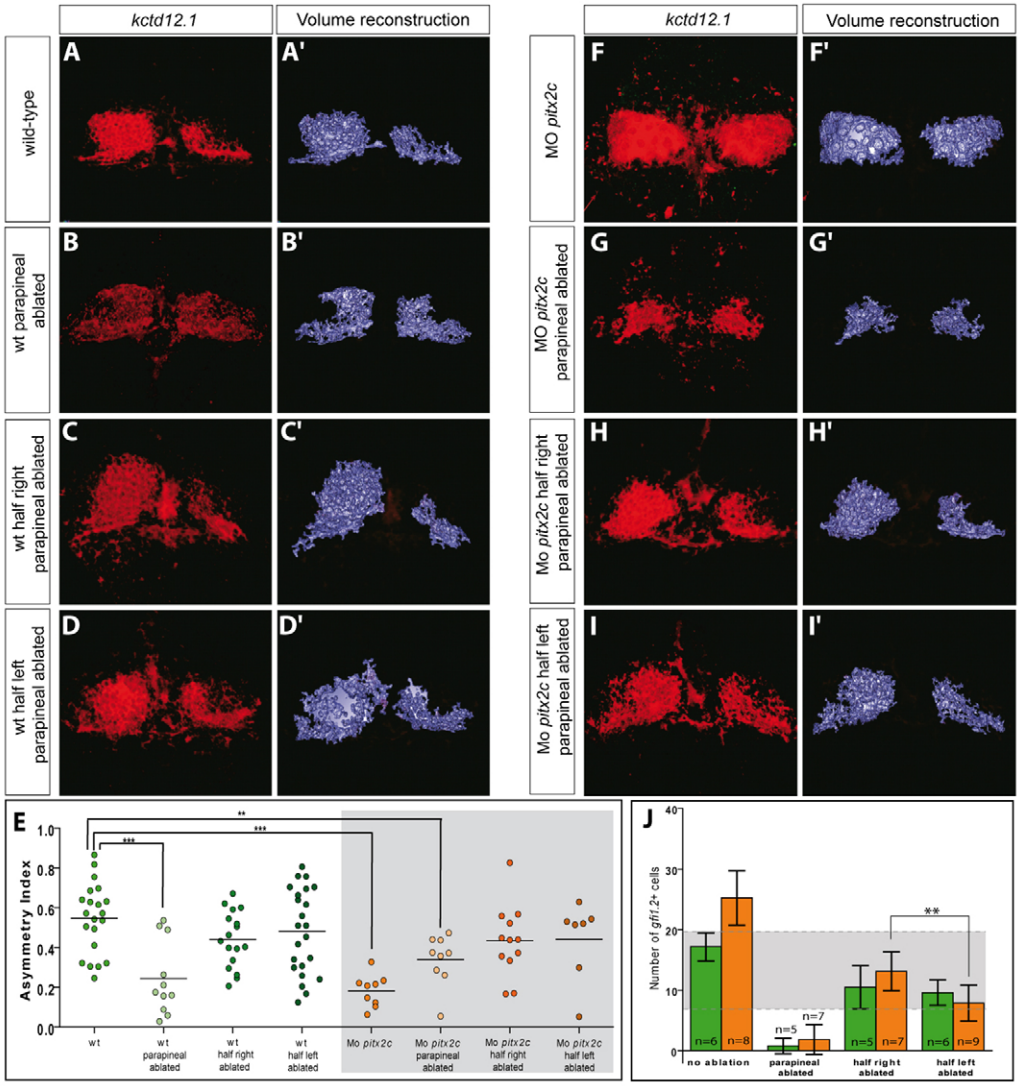

Fig. 5. Restricting parapineal cell number rescues habenular asymmetry. (A-D) Single confocal sections of the epithalamus showing *in situ* hybridisation against *kctd12.1* in wild-type embryos at 72 hpf with no ablation (A), complete parapineal ablation (B) or partial ablation of the right (C) or left (D) half of the parapineal anlage. Although complete parapineal ablation induces right isomerisation of *kctd12.1* expression, no differences are detected in partial ablations. (A′-D′) 3D renderings of volumes of *kctd12.1* expression in the habenulae of the respective confocal acquisition sets. (E) Asymmetry index (AI) with regard to the volume of *kctd12.1* expression for individual wild-type (wt) or morphant embryos with complete or partial parapineal ablations. Horizontal black line represents the median AI for each context. Although complete ablation of the parapineal renders the expression of *kctd12.1* significantly less asymmetric, partial ablation in *pitx2c* morphants restores asymmetry; ***P*<0.01; ****P*<0.001 using a *t*-test. (F-I) Single confocal sections of the epithalamus showing *in situ* hybridisation against *kctd12.1* in *pitx2c* morphant embryos at 72 hpf with no ablation (F), complete parapineal ablation (G) or partial ablation of the right (H) or left (I) half of the parapineal anlage. Although *pitx2c* morphants display left isomerisation of *kctd12.1* expression and complete parapineal ablation induces right isomerisation, partial ablations return the expression pattern of *kctd12.1* to a wild-type pattern. (F′-I′) 3D renderings of volumes of *kctd12.1* expression in the habenulae of the respective confocal acquisition sets. (J) Counts of cells expressing *gfi1.2* in control (green) and *pitx2c* morphant (orange) embryos having undergone no ablation, complete parapineal ablation or partial ablation of the right or left half of the parapineal anlage immediately prior to parapineal migration. Partial ablations in *pitx2c* morphants produce residual parapineals whose cell counts falls within the range sufficient for imposing correct habenular asymmetry in wild-type embryos (highlighted in grey). Although left and right partial ablation in wild-type embryos produces residual parapineals with similar numbers of cells, significantly more parapineal cells remain after partial right than partial left ablations in *pitx2c* morphants. Error bars represent s.d; ***P*<0.01 using a *t*-test. Embryos are viewed dorsally with the anterior towards the top.

of L/R asymmetry in the zebrafish epithalamus. Intriguingly, in this context Pitx2c appears to act via negative feedback against Nodal activity. It waits to be seen if a similar role for Pitx2 exists in other models of L/R asymmetry.

MATERIALS AND METHODS

Fish lines and maintenance

Embryos were raised and staged according to standard protocols (Kimmel et al., 1995). The transgenic lines *Tg(foxd3:GFP)*^{zf15}, *Et(krt4:EGFP)*^{sqet11} and *TgBAC(flh:flh-Kaede)*^{vu376} have been described previously (Gilmour et al., 2002; Choo et al., 2006; Clanton et al., 2013). For later-staged embryos, PTU was used to block the formation of pigment.

In situ hybridisation and antibody labelling

Antisense probes for *kctd8*, *kctd12.1*, *kctd12.2* (Gamse et al., 2003; Gamse et al., 2005), *nrp1a* (Kuan et al., 2007), *brn3a* (Aizawa et al., 2005), *gfi1.2* (Dufourcq et al., 2004), *lefty1* (Thisse and Thisse, 1999), *southpaw* (Long et al., 2003) and *pitx2* (Essner et al., 2000) were generated using standard

procedures. Immunohistochemical stainings were performed as previously described (Masai et al., 1997), using either anti-GFP (Torrey Pines Biolabs) or anti-acetylated tubulin (Sigma) as primary antibodies with the appropriate Alexa Fluor 488-conjugated secondary antibody (Molecular Probes). For nuclear staining, embryos were incubated in ToPro (Molecular Probes).

Volumetric analysis

To quantify volumes, *in situ* hybridisation in control and morphant embryos was performed with Fast-Red (Sigma). Confocal stacks were generated from single sections every 0.18 µm, and volumes from each stack were rendered using Volocity 3D Image Analysis Software. To determine the asymmetry index (AI) for individual embryos, the volume of the left (L) minus the right (R) expression domain was divided by the sum of both left and right volumes, i.e. (L–R)/(L+R). Student's *t*-test was performed using Prism 5 software to compare AI values between datasets (GraphPad Software).

Imaging

For all fluorescent labelling on fixed tissues, embryos were mounted in glycerol and imaged using a Leica SP5 confocal microscope with a 63 oil-immersion objective. For time-lapse analysis, embryos were mounted in 0.8% low melting point agarose and imaged on a Zeiss LSM 710 confocal microscope. To facilitate analysis, time-lapse experiments were performed in embryos carrying a *Tg(foxd3:GFP)*^{zf15} transgene and injected with Histone2B:RFP mRNA to label nuclei.

Morpholinos

Morpholino oligonucleotides were designed to target sequences comprising the Pitx2c ATG or a second sequence in the 5′UTR (Gene Tools); a control morpholino, where mis-matches were introduced in the ATG morpholino sequence, was also designed.

Parapineal ablation and SB431542 treatment

Ablation of parapineal precursors was performed in *TgBAC(flh:flh-Kaede)*^{vu376} transgenic embryos using a Leica SP5 multiphoton confocal microscope. Embryos were subsequently grown to the appropriate stage, fixed and labelled by *in situ* hybridisation to assess parapineal cell numbers and habenular asymmetry. Nodal signalling was modulated by treating embryos with the small molecule inhibitor SB431542 from 16 hpf as previously described (Inman et al., 2002; Roussigné et al., 2009).

Acknowledgements

We are grateful to Julie Batut, Catherine Danesin, Véronique Duboc and members of the Blader lab for critical reading of the manuscript, and to Rebecca Burdine, Vladimir Korzh and Darren Gilmour for reagents and fish lines. We also thank Stéphane Relexans for expert fish husbandry.

Competing interests

The authors declare no competing financial interests.

Author contributions

L.G., B.R., M.R. and S.B. performed experiments and constructed transgenic tools. L.G., P.D. and P.B. analysed the data. P.D. and P.B. conceived the study. J.T.G., P.D. and P.B., coordinated the experiments and wrote the manuscript with input from the other authors.

Funding

This work was supported by the Centre national de la recherche scientifique (CNRS), Institut national de la santé et de la recherche médicale (INSERM), Université de Toulouse III (UPS), Fondation l'Association pour la recherche sur le cancer (ARC) [SFI20101201699] and the French Ministère de la Recherche to P.B.; and by a National Institutes of Health/National Institute of Child Health and Human Development (NIH/NICHD) grant [HD054534] to J.T.G. Deposited in PMC for release after 12 months.

Supplementary material

Supplementary material available online at
http://dev.biologists.org/lookup/suppl/doi:10.1242/dev.100305/-/DC1

References

Aizawa, H., Bianco, I. H., Hamaoka, T., Miyashita, T., Uemura, O., Concha, M. L., Russell, C., Wilson, S. W. and Okamoto, H. (2005). Laterotopic representation of left-right information onto the dorso-ventral axis of a zebrafish midbrain target nucleus. *Curr. Biol.* **15**, 238-243.

Baek, S. H., Kioussi, C., Briata, P., Wang, D., Nguyen, H. D., Ohgi, K. A., Glass, C. K., Wynshaw-Boris, A., Rose, D. W. and Rosenfeld, M. G. (2003). Regulated subset of G1 growth-control genes in response to derepression by the Wnt pathway. *Proc. Natl. Acad. Sci. USA* **100**, 3245-3250.

Bianco, I. H., Carl, M., Russell, C., Clarke, J. D. and Wilson, S. W. (2008). Brain asymmetry is encoded at the level of axon terminal morphology. *Neural Dev.* **3**, 9.

Bohnsack, B. L., Kasprick, D. S., Kish, P. E., Goldman, D. and Kahana, A. (2012). A zebrafish model of axenfeld-rieger syndrome reveals that pitx2 regulation by retinoic acid is essential for ocular and craniofacial development. *Invest. Ophthalmol. Vis. Sci.* **53**, 7-22.

Choo, B. G., Kondrichin, I., Parinov, S., Emelyanov, A., Go, W., Toh, W. C. and Korzh, V. (2006). Zebrafish transgenic Enhancer TRAP line database (ZETRAP). *BMC Dev. Biol.* **6**, 5.

Clanton, J. A., Hope, K. D. and Gamse, J. T. (2013). Fgf signaling governs cell fate in the zebrafish pineal complex. *Development* **140**, 323-332.

Concha, M. L. and Wilson, S. W. (2001). Asymmetry in the epithalamus of vertebrates. *J. Anat.* **199**, 63-84.

Concha, M. L., Burdine, R. D., Russell, C., Schier, A. F. and Wilson, S. W. (2000). A nodal signaling pathway regulates the laterality of neuroanatomical asymmetries in the zebrafish forebrain. *Neuron* **28**, 399-409.

Concha, M. L., Russell, C., Regan, J. C., Tawk, M., Sidi, S., Gilmour, D. T., Kapsimali, M., Sumoy, L., Goldstone, K., Amaya, E. et al. (2003). Local tissue interactions across the dorsal midline of the forebrain establish CNS laterality. *Neuron* **39**, 423-438.

Dufourcq, P., Rastegar, S., Strähle, U. and Blader, P. (2004). Parapineal specific expression of gfi1 in the zebrafish epithalamus. *Gene Expr. Patterns* **4**, 53-57.

Essner, J. J., Branford, W. W., Zhang, J. and Yost, H. J. (2000). Mesendoderm and left-right brain, heart and gut development are differentially regulated by pitx2 isoforms. *Development* **127**, 1081-1093.

Gamse, J. T., Shen, Y. C., Thisse, C., Thisse, B., Raymond, P. A., Halpern, M. E. and Liang, J. O. (2002). Otx5 regulates genes that show circadian expression in the zebrafish pineal complex. *Nat. Genet.* **30**, 117-121.

Gamse, J. T., Thisse, C., Thisse, B. and Halpern, M. E. (2003). The parapineal mediates left-right asymmetry in the zebrafish diencephalon. *Development* **130**, 1059-1068.

Gamse, J. T., Kuan, Y. S., Macurak, M., Brösamle, C., Thisse, B., Thisse, C. and Halpern, M. E. (2005). Directional asymmetry of the zebrafish epithalamus guides dorsoventral innervation of the midbrain target. *Development* **132**, 4869-4881.

Gilmour, D. T., Maischein, H. M. and Nüsslein-Volhard, C. (2002). Migration and function of a glial subtype in the vertebrate peripheral nervous system. *Neuron* **34**, 577-588.

Huang, Y., Guigon, C. J., Fan, J., Cheng, S. Y. and Zhu, G. Z. (2010). Pituitary homeobox 2 (PITX2) promotes thyroid carcinogenesis by activation of cyclin D2. *Cell Cycle* **9**, 1333-1341.

Inman, G. J., Nicolás, F. J., Callahan, J. F., Harling, J. D., Gaster, L. M., Reith, A. D., Laping, N. J. and Hill, C. S. (2002). SB-431542 is a potent and specific inhibitor of transforming growth factor-beta superfamily type I activin receptor-like kinase (ALK) receptors ALK4, ALK5, and ALK7. *Mol. Pharmacol.* **62**, 65-74.

Kimmel, C. B., Ballard, W. W., Kimmel, S. R., Ullmann, B. and Schilling, T. F. (1995). Stages of embryonic development of the zebrafish. *Dev. Dyn.* **203**, 253-310.

Kioussi, C., Briata, P., Baek, S. H., Rose, D. W., Hamblet, N. S., Herman, T., Ohgi, K. A., Lin, C., Gleiberman, A., Wang, J. et al. (2002). Identification of a Wnt/Dvl/beta-Catenin → Pitx2 pathway mediating cell-type-specific proliferation during development. *Cell* **111**, 673-685.

Kitamura, K., Miura, H., Miyagawa-Tomita, S., Yanazawa, M., Katoh-Fukui, Y., Suzuki, R., Ohuchi, H., Suehiro, A., Motegi, Y., Nakahara, Y. et al. (1999). Mouse Pitx2 deficiency leads to anomalies of the ventral body wall, heart, extra- and periocular mesoderm and right pulmonary isomerism. *Development* **126**, 5749-5758.

Kuan, Y. S., Yu, H. H., Moens, C. B. and Halpern, M. E. (2007). Neuropilin asymmetry mediates a left-right difference in habenular connectivity. *Development* **134**, 857-865.

Liang, J. O., Etheridge, A., Hantsoo, L., Rubinstein, A. L., Nowak, S. J., Izpisúa Belmonte, J. C. and Halpern, M. E. (2000). Asymmetric nodal signaling in the zebrafish diencephalon positions the pineal organ. *Development* **127**, 5101-5112.

Lin, C. R., Kioussi, C., O'Connell, S., Briata, P., Szeto, D., Liu, F., Izpisúa-Belmonte, J. C. and Rosenfeld, M. G. (1999). Pitx2 regulates lung asymmetry, cardiac positioning and pituitary and tooth morphogenesis. *Nature* **401**, 279-282.

Liu, Y. and Semina, E. V. (2012). pitx2 Deficiency results in abnormal ocular and craniofacial development in zebrafish. *PLoS ONE* **7**, e30896.

Liu, C., Liu, W., Lu, M. F., Brown, N. A. and Martin, J. F. (2001). Regulation of left-right asymmetry by thresholds of Pitx2c activity. *Development* **128**, 2039-2048.

Long, S., Ahmad, N. and Rebagliati, M. (2003). The zebrafish nodal-related gene southpaw is required for visceral and diencephalic left-right asymmetry. *Development* **130**, 2303-2316.

Lu, M. F., Pressman, C., Dyer, R., Johnson, R. L. and Martin, J. F. (1999). Function of Rieger syndrome gene in left-right asymmetry and craniofacial development. *Nature* **401**, 276-278.

Masai, I., Heisenberg, C. P., Barth, K. A., Macdonald, R., Adamek, S. and Wilson, S. W. (1997). floating head and masterblind regulate neuronal patterning in the roof of the forebrain. *Neuron* **18**, 43-57.

Paylakhi, S. H., Fan, J. B., Mehrabian, M., Sadeghizadeh, M., Yazdani, S., Katanforoush, A., Kanavi, M. R., Ronaghi, M. and Elahi, E. (2011). Effect of

PITX2 knockdown on transcriptome of primary human trabecular meshwork cell cultures. *Mol. Vis.* **17**, 1209-1221.

Regan, J. C., Concha, M. L., Roussigné, M., Russell, C. and Wilson, S. W. (2009). An Fgf8-dependent bistable cell migratory event establishes CNS asymmetry. *Neuron* **61**, 27-34.

Roussigné, M., Bianco, I. H., Wilson, S. W. and Blader, P. (2009). Nodal signalling imposes left-right asymmetry upon neurogenesis in the habenular nuclei. *Development* **136**, 1549-1557.

Roussigné, M., Blader, P. and Wilson, S. W. (2012). Breaking symmetry: the zebrafish as a model for understanding left-right asymmetry in the developing brain. *Dev. Neurobiol.* **72**, 269-281.

Semina, E. V., Reiter, R., Leysens, N. J., Alward, W. L., Small, K. W., Datson, N. A., Siegel-Bartelt, J., Bierke-Nelson, D., Bitoun, P., Zabel, B. U. et al. (1996). Cloning and characterization of a novel bicoid-related homeobox transcription factor gene, RIEG, involved in Rieger syndrome. *Nat. Genet.* **14**, 392-399.

Shiratori, H., Sakuma, R., Watanabe, M., Hashiguchi, H., Mochida, K., Sakai, Y., Nishino, J., Saijoh, Y., Whitman, M. and Hamada, H. (2001). Two-step regulation of left-right asymmetric expression of Pitx2: initiation by nodal signaling and maintenance by Nkx2. *Mol. Cell* **7**, 137-149.

Thisse, C. and Thisse, B. (1999). Antivin, a novel and divergent member of the TGFbeta superfamily, negatively regulates mesoderm induction. *Development* **126**, 229-240.

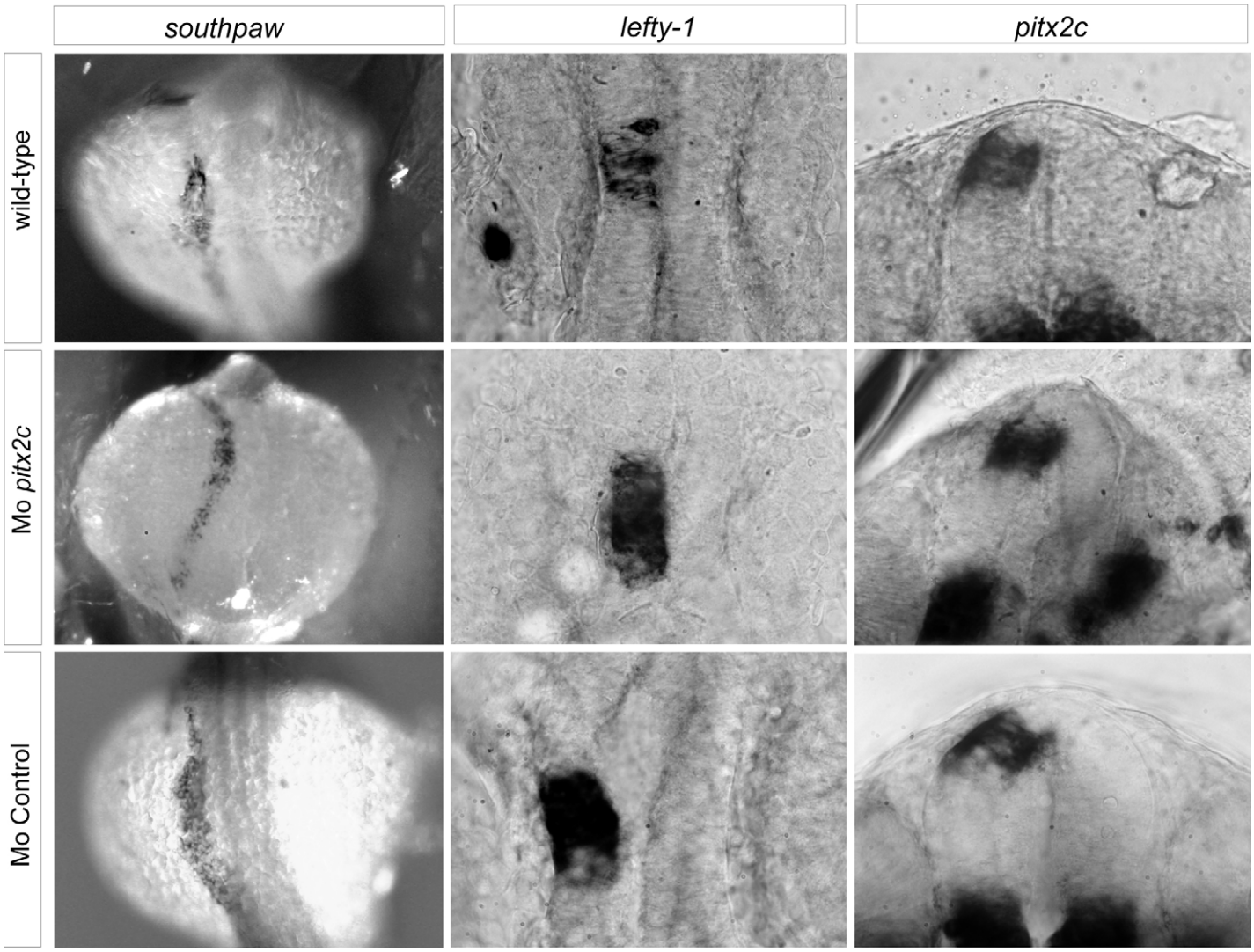

Supplementary Figure 1.

No changes are detected in the expression of the Nodal family gene *southpaw* in the left lateral plate mesoderm at 18 hpf, or in the expression of *pitx2c* and the Nodal feedback inhibitor *lefty1* in the left dorsal diencephalons at 24 hpf in *pitx2c* morphants relative to wild-type and control morphants suggesting that the establishment of L/R asymmetry is not generally affected.

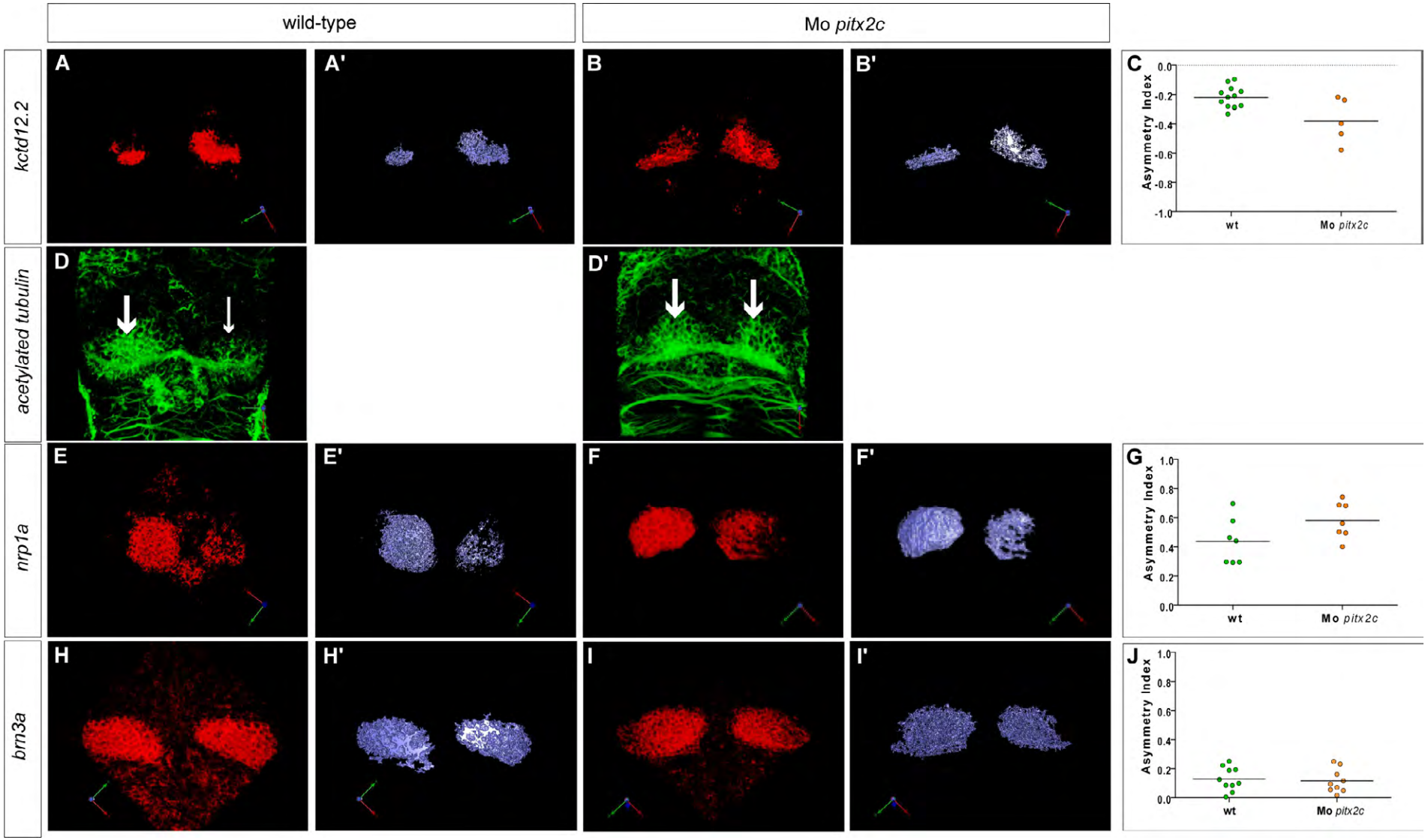
wild-type
Mo pitx2c
kctd12.2
acetylated tubulin
nrp1a
brn3a
A
A'
B
B'
C
D
D'
E
E'
F
F'
G
H
H'
I
I'
J
Asymmetry Index
0.0
-0.2
-0.4
-0.6
-0.8
-1.0
wt
Mo pitx2c
1.0
0.8
0.6
0.4
0.2
0.0

Supplementary Figure 2.

(A, B) Single confocal sections of the epithalamus showing *in situ* hybridisation against *kctd12.2* in wild-type and *pitx2c* morphant embryos at 72 hpf.

(A', B') 3D renderings of volumes of *kctd12.2* expression in the habenulae of the respective confocal acquisition sets.

(C) Asymmetry index (AI) with regard to the volume of *kctd12.2* expression for individual wild-type or *pitx2c* morphant embryos. Horizontal black line represents the median AI for each context: note that the AI is negative because the asymmetry is biased to the right. No significant difference between wild-type or *pitx2c* morphant embryos is detected.

(D, D') Single confocal sections through the epithalamus showing the habenular neuropil detected by immunostaining against acetylated tubulin at 72 hpf. While the neuropil of wild-type embryos is asymmetric with a left bias (large versus small arrows), symmetric anti-acetylated tubulin staining is detected in *pitx2c* morphant embryos (two large arrows).

(E, F) Single confocal sections of the epithalamus showing *in situ* hybridisation against *nrp1a* in wild-type and *pitx2c* morphant embryos at 72 hpf.

(E', F') 3D renderings of volumes of *nrp1a* expression in the habenulae of the respective confocal acquisition sets.

(G) Asymmetry index with regard to the volume of *nrp1a* expression for individual wild-type or *pitx2c* morphant embryos. Horizontal black line represents the median AI for each context . No significant difference between wild-type or *pitx2c* morphant embryos is detected.

(H, I) Single confocal sections of the epithalamus showing *in situ* hybridisation against *brn3a* in wild-type and *pitx2c* morphant embryos at 72 hpf.

(H', I') 3D renderings of volumes of *brn3a* expression in the habenulae of the respective confocal acquisition sets.

(J) Asymmetry index with regard to the volume of *brn3a* expression for individual wild-type or *pitx2c* morphant embryos. Horizontal black line represents the median AI, which are in both contexts close to zero reflecting that they are virtually symmetric. No significant difference between wild-type or *pitx2c* morphant embryos is detected.

Embryos are view dorsally with the anterior to the top.

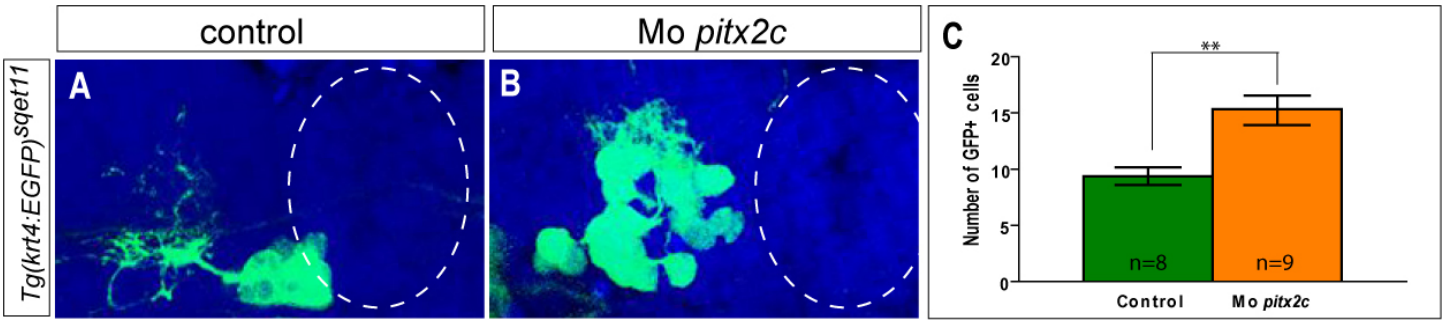

Supplementary Figure 3.

(A,B) Confocal projections showing the expression of GFP from the *Et(krt4:EGFP)*^{sqet11} transgene in control and *pitx2c* morphant embryos at 72 hpf. The outline of the pineal gland is highlight with a dotted line.

(C) Counts of cell expressing GFP in control and *pitx2c* morphants. The number of GFP-positive cells is significantly increased in the morphant context; **P<0.01 using a t-test. Error bars represent s.d.

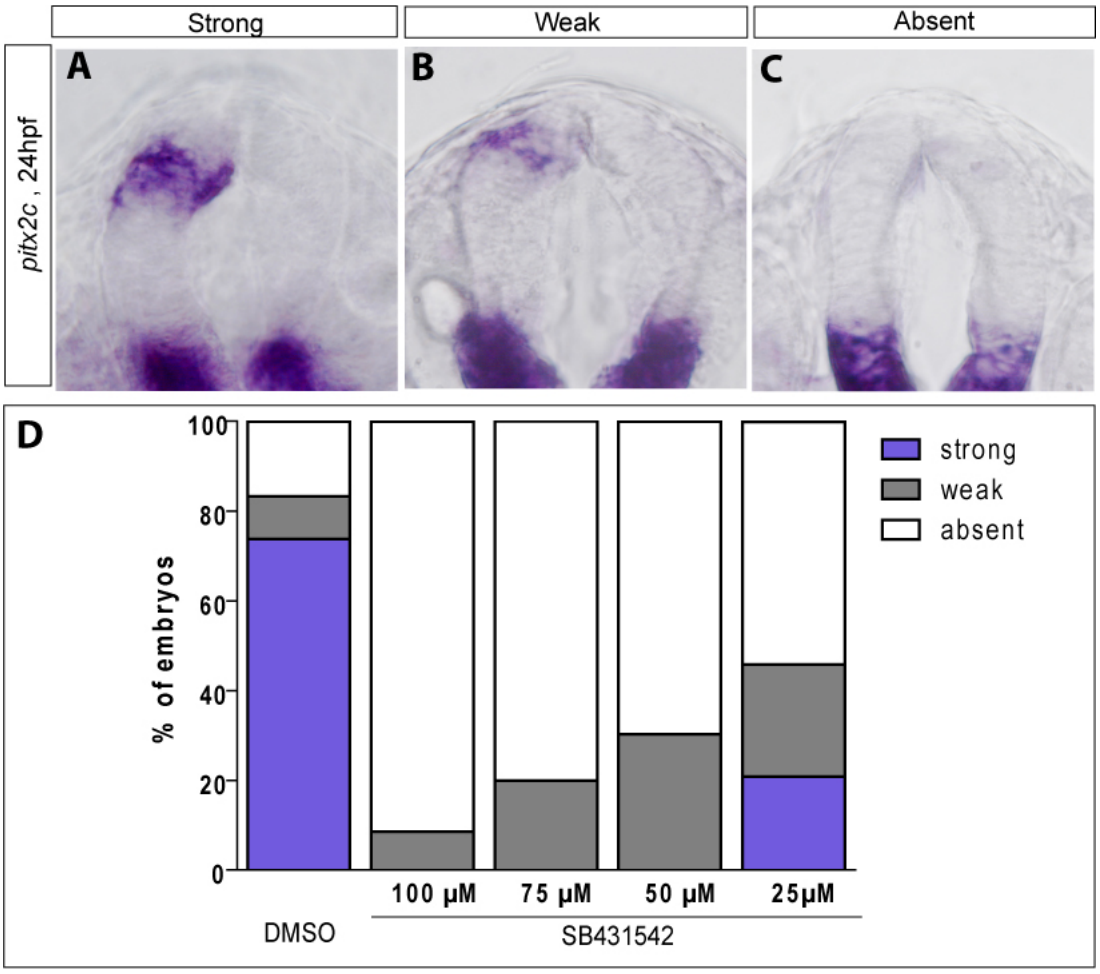

Supplementary Figure 4.

(A-C) Frontal view of the epithalamus showing *in situ* hybridisation against *pitx2c* at 24 hpf. Expression can be qualified as Strong (A), Weak (B) or Absent (C).

(D) Quantification of *pitx2c* expression classes presented in (A-C) in mock-treated and embryos treated with varying concentrations of SB431542 from 16 to 72 hpf .

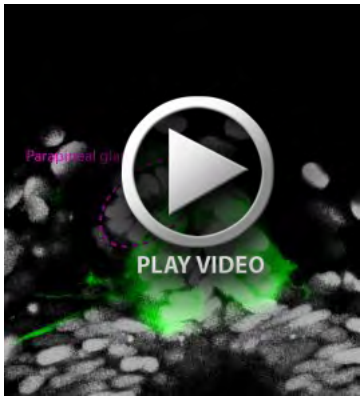

Movie 1.

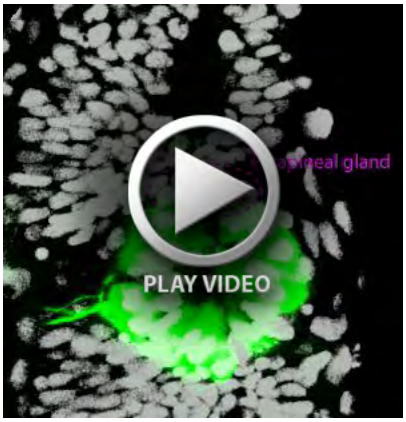

Movie 2.

Movie 3.

Supplementary Movies 1 (wild-type), 2 (Mo *pitx2c*) and 3 (Mo *pitx2c*).

Time-lapse movies showing the migrating parapineal in wild-type and a *pitx2c* morphant embryo carrying the *Tg(foxd3:GFP)*^{zf15} transgene; nuclei are labelled with Histone2B:RFP and false coloured in grey. The movies were generated from a projection of 3 Z-sections at each time point. While in the wild-type embryo one cell division is noted during the movie, in the Mo *pitx2c* embryos 4 or 6 divisions can be seen, respectively; divisions are highlighted with purple arrows that appear to split at the time of division. Films were initiated between 24-26 hpf and the initial frame is annotated to indicate the parapineal (dotted line).